Advances in MgO Nanoparticle Synthesis: Pathways to Future Antimicrobial Applications

Yarilyn Cedeño-Mattei, Sonia Bailón-Ruiz
Department of Chemistry and Physics,
University of Puerto Rico at Ponce

Resumen

Las nanopartículas de óxido de magnesio, MgO, han captado una atención significativa en los últimos años debido a sus prometedoras propiedades antimicrobianas y posibles aplicaciones en diversos campos. Estas nanopartículas exhiben características fisicoquímicas únicas, incluyendo una alta razón superficie-volumen y una estabilidad excepcional. Estos atributos permiten a las nanopartículas de MgO interactuar efectivamente con microorganismos, convirtiéndolas en agentes potentes contra una amplia gama de bacterias, hongos e incluso algunos virus. La actividad antimicrobiana de las nanopartículas de MgO se atribuye principalmente a su capacidad para producir especies reactivas de oxígeno (ROS) al entrar en contacto con la humedad o fluidos biológicos. Estos ROS, como los iones superóxido y los radicales hidroxilo, infligen estrés oxidativo en las células microbianas, lo que lleva a daños en la membrana, desnaturalización de proteínas y alteración del ADN. Además, las nanopartículas de MgO han mostrado baja toxicidad hacia las células mamíferas, lo que las convierte en candidatas atractivas para aplicaciones biomédicas, incluyendo la curación de heridas, sistemas de administración de fármacos y recubrimientos de superficies para dispositivos médicos. El tamaño de cristal de las nanopartículas de MgO juega un papel crucial en sus propiedades antimicrobianas, ya que las partículas más pequeñas tienden a exhibir una actividad antimicrobiana mejorada debido a su mayor superficie, que facilita una mayor interacción con los microorganismos. En general, las nanopartículas de MgO poseen un inmenso potencial como agentes antimicrobianos, ofreciendo un enfoque novedoso contra las infecciones microbianas. Basado en lo anterior, el presente artículo describe el desarrollo de una ruta de síntesis reproducible y costo-efectiva para el MgO a escala nanométrica en función del tamaño del cristal. El MgO a escala nanométrica se produjo mediante la descomposición térmica de un precursor hidrato-carbonato de magnesio (hidromagnesita) sintetizado en fase acuosa y en una mezcla de etanol: agua 80:20. La formación de la fase de MgO, con un tamaño promedio de cristalito entre 14.7 y 25.9 nm, fue evidenciada por análisis de Difracción de Rayos X (XRD), Espectroscopia Infrarroja (FT-IR) y Microscopía Electrónica de Transmisión (TEM). Análisis termogravimétricos se utilizaron para monitorear el porcentaje de pérdida de peso y la evolución desde el precursor hasta la estructura deseada.

Palabras clave: óxido de magnesio, nanopartículas, propiedades antimicrobianas

Abstract

Magnesium oxide (MgO) nanoparticles (NPs) have gathered significant attention in recent years due to their promising antimicrobial properties and potential applications in various fields. These nanoparticles exhibit unique physicochemical characteristics, including a high surface area-to-volume ratio and exceptional stability. These attributes enable MgO nanoparticles to interact effectively with microorganisms, making them potent agents against a wide range of bacteria, fungi, and even some viruses. The antimicrobial activity of MgO nanoparticles is primarily attributed to their ability to produce reactive oxygen species (ROS) upon contact with moisture or biological fluids. These ROS, such as superoxide ions and hydroxyl radicals, inflict oxidative stress on microbial cells, leading to membrane damage, protein denaturation, and DNA disruption. Furthermore, MgO nanoparticles have shown low toxicity towards mammalian cells, making them attractive candidates for biomedical applications, including wound healing, drug delivery systems, and surface coatings for medical devices. The crystal size of MgO nanoparticles plays a crucial role in their antimicrobial properties, as smaller particles tend to exhibit enhanced antimicrobial activity due to their larger surface area, which facilitates greater interaction with microorganisms. Overall, MgO nanoparticles possess immense potential as antimicrobial agents, offering a novel approach against microbial infections. Based on the above, the present paper describes the development of a reproducible and cost-effective size-controlled synthesis route for nanoscale MgO as a function of crystal size. Nanoscale MgO was produced through the thermal decomposition of Mg-carbonate hydrate precursor (hydromagnesite) synthesized in aqueous phase and 80:20 ethanol:water mixture. The formation of the MgO phase, with an average crystallite size between 14.7 and 25.9 nm, was evidenced by X-Ray Diffraction (XRD), Infrared Spectroscopy (FT-IR), and Transmission Electron Microscopy (TEM) analyses. Thermogravimetric analyses were used to monitoring the weight loss percentage and the evolution from the precursor to the desired structure.

Keywords: magnesium oxide, nanoparticles, antimicrobial properties

1. Introduction

Each year in the United States, foodborne diseases sicken millions of people and cause thousands of deaths according to data from the Centers for Disease Control and Prevention. The CDC estimates that 48 million Americans get sick, 128,000 are hospitalized, and 3,000 die of foodborne diseases annually (CDC, 2023). There are 31 known pathogens that cause foodborne illness (*Burden of Foodborne Illness*, 2023). The three most commonly known pathogens that cause foodborne illness are norovirus, salmonella, and clostridium perfringens. Specifically, norovirus accounts for roughly 20 million cases of acute gastroenteritis each year. Non-typhoidal salmonella causes about 1.35 million infections, 26,500 hospitalizations, and 420 deaths annually in the United States. Clostridium perfringens causes an estimated 1 million cases of foodborne illness and over 300 deaths each year. Additionally, campylobacter causes over 1.3 million cases of food poisoning annually.

Foodborne illness places a large burden on society through both medical costs and lost productivity. Healthcare costs and lost productivity from major known pathogens alone are estimated to exceed $15.5 billion every year in the United States (*USDA ERS - Cost Estimates of Foodborne Illnesses*, 2023). The total burden is likely much higher when accounting for unreported cases. Reducing illness caused by food pathogens requires vigilance by food producers, processors, and consumers to prevent contamination throughout the food system. Continued surveillance work by the CDC is vital to track trends, identify disease clusters, and guide policy efforts aimed at reducing the substantial public health impacts of food poisoning in America (*CDC and Food Safety | CDC*, 2023). Further progress remains needed to safeguard citizens from preventable harms linked to contaminated foods.

Magnesium oxide, a versatile inorganic compound, has gathered significant attention in recent years, particularly at the nanoscale, due to its promising applications in various fields including medicine (Abdul-Hamead et al., 2021; Nejati et al., 2022), environmental science (Gao et al., 2017; Li et al., 2020), and materials engineering. This growing interest is partly attributed to the unique properties that emerge at the nanoscale, which are distinct from those observed in its bulk counterpart. In the realm of antimicrobial applications (Lin et al., 2020; Vidhya et al., 2021), nanoscale MgO represents a particularly intriguing subject of study. The alarming rise in antibiotic-resistant pathogens has propelled the search for novel antimicrobial agents that can offer effective alternatives to conventional antibiotics (MacLean & San Millan, 2019; Mancuso et al., 2021; Pepi & Focardi, 2021). In this context, MgO NPs have emerged as a candidate of considerable potential, owing to their broad-spectrum antimicrobial activity and distinct mode of action compared to traditional antimicrobial agents.

The antimicrobial efficacy of MgO NPs is believed to be a result of multiple mechanisms. These include the generation of reactive oxygen species, disruption of microbial cell membranes, and the alteration of intracellular pathways (Bhattacharya et al., 2021; Cai et al., 2017). Such multifaceted mechanisms not only contribute to the effectiveness of MgO NPs against a wide range of pathogens, including bacteria, fungi, and viruses but also reduce the likelihood of developing resistance. Moreover, the physicochemical properties of MgO NPs, such as particle size, surface area, and morphology, play a crucial role in determining their antimicrobial potency (Bhattacharya et al., 2019; Lin et al., 2020). Nano-scale dimensions of MgO provide a larger surface area-to-volume ratio, enhancing interactions with microbial cells.

This aspect underlines the importance of synthesizing and characterizing MgO NPs with controlled size and shape to optimize their antimicrobial properties. Despite the promising prospects of MgO NPs as antimicrobial agents, challenges remain in understanding their interaction with biological systems, potential toxicity, and environmental impact. These aspects are critical for translating laboratory findings into practical applications, particularly in medical and environmental contexts.

In this study, specific attention has been devoted to modifying the size of MgO nanoparticles, recognizing that size variation can significantly influence their antimicrobial efficacy and other functional characteristics. We employed various synthesis conditions to control and modify the size and/or shape of the MgO nanoparticles. These modifications were studied to understand their impact on the physical properties of the nanoparticles. It enhances the unders-tandding of MgO nanoparticle synthesis and also opens paths for tailored applications in diverse fields.

2. Experimental

2.1 Synthesis of Magnesium Hydroxide Carbonate Precursor and MgO Nanoparticles

The production of magnesium carbonate hydroxide, commonly known as hydromagnesite, as a precursor, was performed through a modified method initially proposed by (Zhao et al., 2002). This process involves distinct nucleation and aging phases in an aqueous environment (or ethanol: water mixture). Solution-1 comprises 100 mL of 0.3 M $MgCl_2$, whereas Solution-2 contains 100 mL of stoichiometrically balanced Na_2CO_3 and NaOH. Both solutions were concurrently introduced into the reaction vessel and uniformly mixed at 11000 rpm for two minutes, constituting the nucleation phase. Subsequently, the resultant mixture was continuously stirred and heated at 100 °C for one hour (aging phase). Upon completion of the aging period, the precipitate undergoes triple washing with deionized water (or ethanol: water mixture) and was then dried at 80 °C for 24 hours. The formation of hydromagnesite is represented by the following chemical equation:

$$5\,MgCl_2 + 4\,Na_2CO_3 + 2\,NaOH \xrightarrow{\Delta} 4\,MgCO_3.Mg(OH)_2.4H_2O + 10\,NaCl \quad (1)$$

The synthesized magnesium carbonate hydroxide precursor undergoes thermal treatment to facilitate the formation of MgO. This involves a three-stage process (Botha & Strydom, 2001) encompassing dehydration, dehydroxylation, and decarbonation of the precursor, leading to the following reaction:

$$4\,MgCO_3.Mg(OH)_2.4H_2O \xrightarrow{\Delta} 5\,MgO + 5\,H_2O + 4\,CO_2 \quad (2)$$

Botha & Strydom (2001) suggest that the thermal decomposition of hydromagnesite likely occurs in three stages:

Dehydration (removal of water of crystallization):

$$4\,MgCO_3.Mg(OH)_2.4H_2O \rightarrow 4\,MgCO_3.Mg(OH)_2 + 4H_2O \qquad (< 250\,°C) \quad (3)$$

Dehydroxylation (decomposition of magnesium hydroxide to MgO):

$$4\,MgCO_3.Mg(OH)_2 \rightarrow 4\,MgCO_3 + MgO + H_2O \qquad (250 - 350\,°C) \quad (4)$$

Decarbonation (decomposition of magnesium carbonate to MgO):

$$4\,MgCO_3 \rightarrow 4\,MgO + 4\,CO_2 \qquad (>350\,^{\circ}C) \qquad (5)$$

2.2 Modified synthesis procedure

Use of surfactants or polymers: A surfactant, cetyltrimethylammonium bromide (CTAB), and a polymer, polyvinylpyrrolidone (PVP), were used in the synthesis of magnesium oxide as an attempt to modify the crystallite size. The mentioned surfactant or polymer were introduced into the same vessel (Solution-2) with the sodium hydroxide and sodium carbonate solutions during the synthesis procedure.

2.3 Characterization Techniques

X-Ray Diffraction (XRD): This technique serves as a sophisticated, non-invasive method to evaluate the crystalline structure of nanoparticles. By analyzing the diffraction patterns obtained, the average size of the crystallites can be accurately estimated, utilizing Scherrer's equation. A Siemens D 500 powder X-Ray diffractometer using Cu-K□ radiation was used.

Fourier Transform Infrared (FT-IR) Spectroscopy: It is an integral technique in studying the chemical transformation of materials. In this context, FT-IR spectroscopy is applied to monitor and analyze the chemical changes occurring as hydromagnesite is thermally treated to convert into MgO.

Transmission Electron Microscopy (TEM): HR-TEM is a powerful tool for obtaining detailed images and structural information at the atomic or molecular level. The technique involves bombarding the specimen with a beam of high-energy electrons, leading to various signal emissions. These signals, particularly those responsible for creating bright field images and electron diffraction patterns (ED) are critical in elucidating the specimen's detailed structural attributes.

Thermogravimetric Analysis (TGA): TGA is an instrumental technique for measuring the change in a material's weight as it undergoes thermal treatment. This analysis is pivotal in quantifying the weight loss percentage, which is a crucial parameter in understanding the thermal stability and composition of the material.

3. Results and Discussion

3.1 X-Ray Diffraction (XRD) Analyses

Figure 1 shows the XRD patterns of the magnesium carbonate hydroxide precursor synthesized in aqueous solution (100% water), synthesized in aqueous solution in addition to 1 g of PVP, and synthesized in aqueous solution in addition to CTAB at a [CTAB]/[Mg^{2+}] molar ratio of 0.1. The precursor was also synthesized using a 80:20 ethanol: water mixture as solvent. As seen, there is no remarkable difference in the crystallinity of the precursors obtained in aqueous solutions. Moreover, the precursor obtained from the ethanol: water mixture seems to be a totally different and poorly crystalline structure.

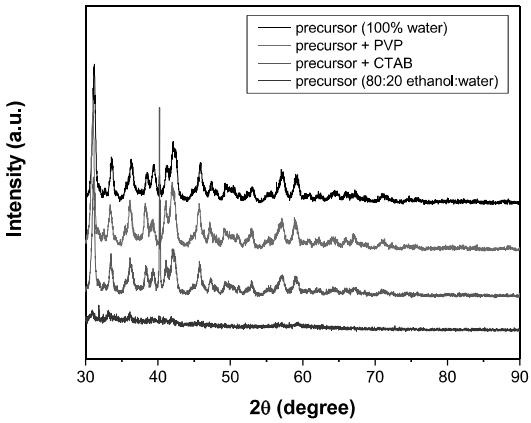

Figure 1: XRD patterns of the synthesized precursors.

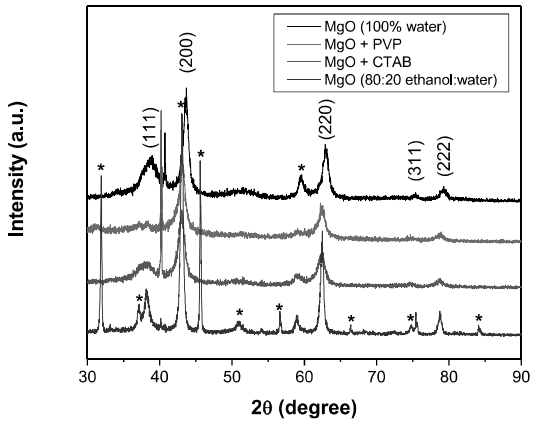

Figure 2: XRD patterns for MgO nanoparticles obtained after thermal treatment of the precursor at 500 °C for 1 hour in air atmosphere.

In order to promote the MgO formation, the one-hour aged hydromagnesite product was thermally treated in air at 500 °C; the corresponding XRD patterns are shown in Figure 2. The presence of diffraction peaks corresponding to the crystallographic planes (111), (200), (220), (311), and (222) of cubic MgO-periclase became evident. The lattice parameter for the sample synthesized after one hour of thermal decomposition was estimated at 4.22 Å, which is in good agreement with the bulk value for MgO (4.21 Å). The average crystallite sizes of MgO, estimated by using the Scherrer's equation, ranged between 14.7–25.1 nm for the samples prepared in aqueous phase (Table 1). The MgO nanoparticles obtained from the precursor synthesized in ethanol: water mixture had an average crystallite size of 25.9 nm. Poorly crystalline structures would require less thermal energy to be converted into the oxide phase and could take advantage of the excess of energy to promote crystal growth. In addition, a secondary phase was detected; its corresponding diffraction peaks are marked with an asterisk (*).

Table 1: Average crystallite size, 'd', for MgO nanoparticles synthesized under different conditions.

Sample	d (nm)
MgO (water 100 %)	14.7
MgO + PVP	15.4
MgO + CTAB	25.1
MgO (80:20 ethanol: water)	25.9

3.2 Fourier Transform Infrared (FT-IR) Spectroscopy

FT-IR measurements confirmed the structure of both, the hydromagnesite precursor and the resulting MgO phase. Figure 3 shows the FT-IR spectra of hydromagnesite produced at an aging time of 1 hour and the MgO resulting after thermal treatment for 1 hour at 500 °C in air. The sharp bands at 1475 and 1420 cm^{-1} corresponds to the CO_3^{2-} asymmetric stretching while the band at 1100 cm^{-1} is attributed to CO_3^{2-} symmetric stretching of hydromagnesite. The bands attributed to carbonate ion decreased considerably after thermal

treatment due to decarbonation of the precursor. The spectrum corresponding to MgO clearly shows an intense band at 540 cm^{-1} that corresponds to the Mg-O vibration.

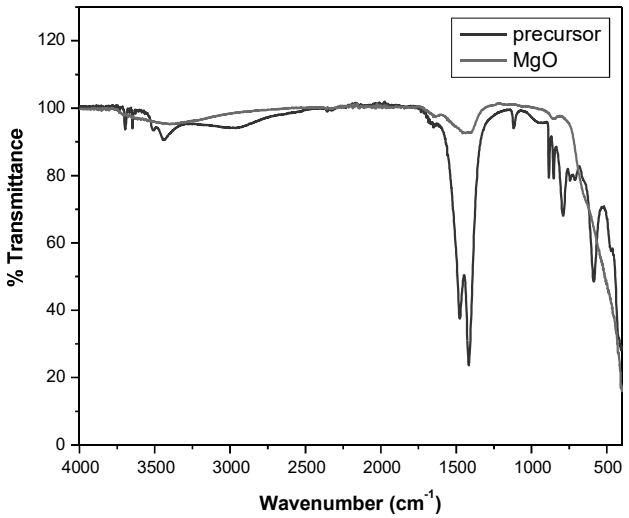

Figure 3: FT-IR spectra of hydromagnesite precursor and MgO nanoparticles after thermal treatment at 500 °C for 1 hour in air atmosphere.

3.3 Transmission Electron Microscopy (TEM) Analyses

TEM, HRTEM images, and ED pattern of 14.7 nm MgO nanoparticles synthesized in aqueous solution are shown in Figure 4. The nanometric nature of the MgO particles and their high crystallinity was evidenced (Figures 4 a-d).

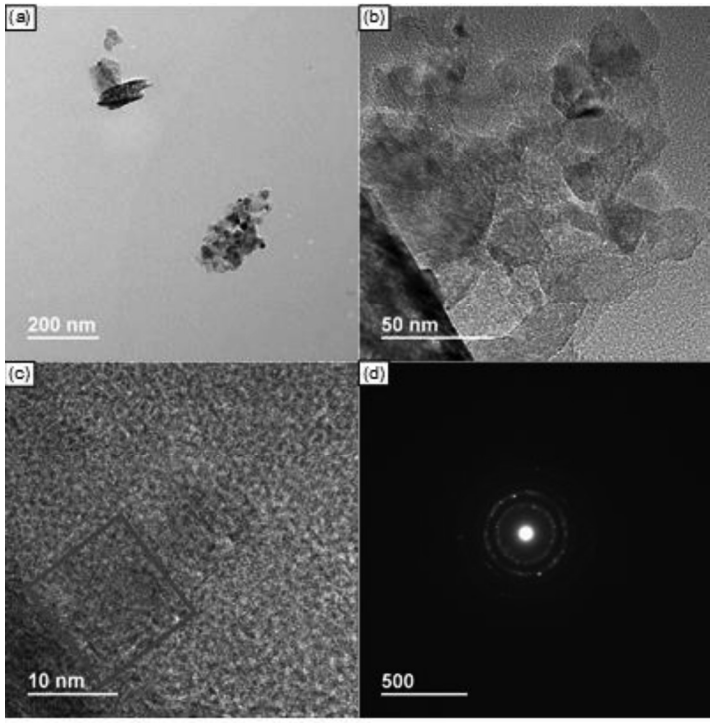

Figure 4: TEM images, (a-c), and electron diffraction pattern, (d), of MgO nanoparticles synthesized in aqueous solution.

Figure 5 corresponds to a TEM image and an ED pattern of MgO produced using 80:20 ethanol: water mixture. The TEM images revealed a mixture of rounded and square-shaped particles and bigger sizes when compared to its counterpart prepared in aqueous solution. It is important to notice that the nanoparticle's shape also affects the MgO properties.

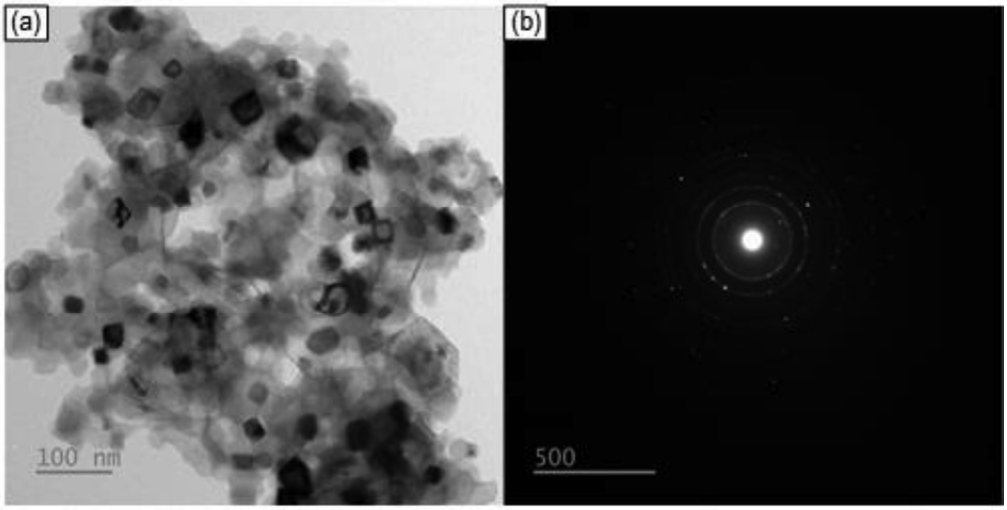

Figure 5: TEM image, (a), and electron diffraction pattern, (b), of MgO nanoparticles synthesized in 80:20 ethanol: water solution.

3.4 TG-DTG Measurements

Figure 6 shows the TG-DTG profiles of hydromagnesite precursor synthesized in aqueous solution (100% water), synthesized in aqueous solution in addition to 1 g of PVP, and synthesized in aqueous solution in addition to CTAB at a [CTAB]/[Mg^{2+}] molar ratio of 0.1. The TG-DTG profile of the precursor synthesized using an 80:20 ethanol: water mixture as solvent is also presented. In all samples synthesized using water as solvent (with and without surfactants or polymers), weight losses of 60 % occurred around 410 ºC, which is higher than the theoretical weight loss of 56.9 % expected after dehydration, dehydroxylation, and decarbonation processes of the intermediate phases. The larger weight loss could be attributed to the presence of moisture in the sample. The precursors produced in presence of PVP and CTAB exhibited a weight loss comparable to hydromagnesite synthesized in their absence. It is possible that the surfactants were not covalently adsorbed onto the precursor surface and were thermally decomposed during heating. Furthermore, the precursor synthetized in 80:20 ethanol: water mixture was conducive to a drop in temperature required for the oxide formation (only 350°C was required); the weight loss for this sample was estimated at 55%. It could be attributed to the formation of a precursor with a stoichiometry different than hydromagnesite, e. g. Mg alkoxide, which decomposes at temperatures below 350 °C as referenced by (Jung et al., 2003). That kind of compound, alkoxides, could also led to the formation of nanosized materials.

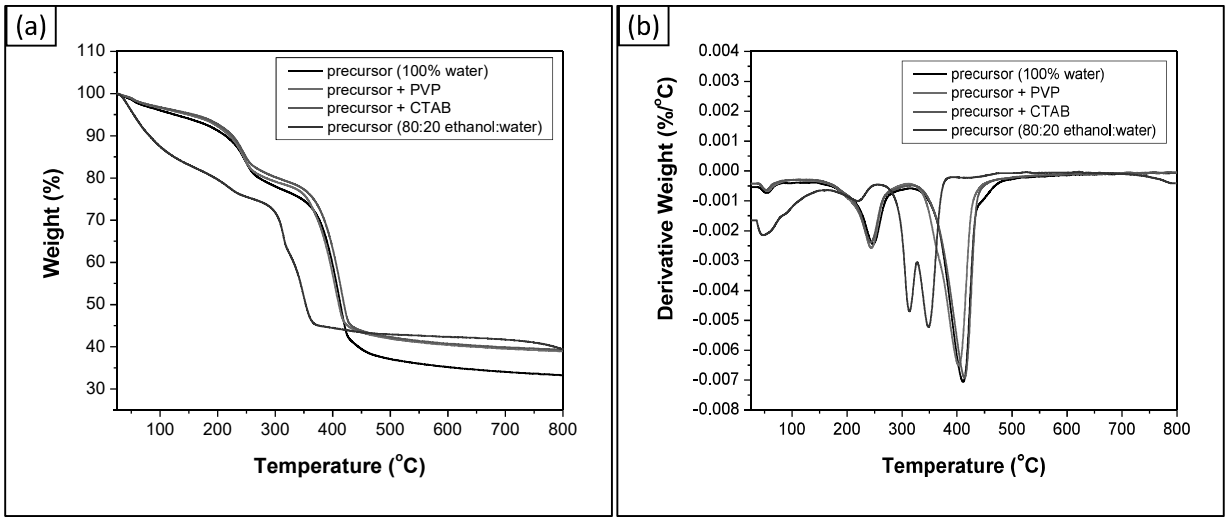

Figure 6: TGA-DTG profiles of precursors synthetized under different conditions.

4. Conclusions

In this study, we successfully synthesized magnesium oxide nanoparticles within the size range of 14.7–25.9 nm. The synthesis process was meticulously analyzed, with particular focus on the influence of solvents, surfactants, and polymers. Our findings reveal that the solvent used in the two-step synthesis process plays a pivotal role in determining the precursor's characteristics, which in turn significantly influences the size, shape, and composition of the resultant MgO nanoparticles.

Through comprehensive X-Ray Diffraction, FT-IR, and TEM analyses, we confirmed the formation of the desired nanoparticle structure. This confirmation not only validates our synthesis method but also opens up new avenues for the application of these nanoparticles in antimicrobial treatments. The nanometric nature of the particles obtained in this research is particularly noteworthy as it suggests its potential effectiveness in combating microbial pathogens. In conclusion, the successful synthesis of MgO nanoparticles within a controlled size range, as demonstrated in this study, represents a significant step forward in the field of nanomaterials. This advancement not only contributes to the growing body of knowledge in nanoparticle synthesis but also opens up exciting possibilities for their application in addressing pressing public health issues.

5. Acknowledgements

This material is based upon work supported by the “Propuestas de Investigación y Creación Académicas 2022-2023”, from the University of Puerto Rico at Ponce, the National Science
Foundation under Grant No. 2313252, and the Department of Defense/US Army No. W911NF-21-1-0206. TEM analyses were performed at the National High Magnetic Field Laboratory, supported by National Science Foundation Cooperative Agreement No. DMR-2128556 and the State of Florida.

We thank the support of Dr. Tessie H. Cruz-Rivera (Chair of the UPRP), and the Laboratory of Investigation in Nanotechnology and Characterization (LINC) of the Department of Chemistry and Physics.

References

Abdul-Hamead, A. A., Othman, F. M., & Fakhri, M. A. (2021). Preparation of MgO–MnO_2 nanocomposite particles for cholesterol sensors. *Journal of Materials Science: Materials in Electronics*, *32*(11), 15523–15532. https://doi.org/10.1007/s10854-021-06102

Bhattacharya, P., Dey, A., & Neogi, S. (2021). An insight into the mechanism of antibacterial activity by magnesium oxide nanoparticles. *Journal of Materials Chemistry B*, *9*(26), 5329–5339.https://doi.org/10.1039/D1TB00875G

Bhattacharya, P., Swain, S., Giri, L., & Neogi, S. (2019). Fabrication of magnesium oxide nanoparticles by solvent alteration and their bactericidal applications. *Journal of Materials Chemistry B*, *7*(26), 4141–4152. https://doi.org/10.1039/C9TB00782B

Botha, A., & Strydom, C. A. (2001). Preparation of a magnesium hydroxy carbonate from magnesium hydroxide. *Hydrometallurgy*, *62*(3), 175–183. https://doi.org/10.1016/S0304-386X(01)00197-9

Burden of Foodborne Illness: Findings | Estimates of Foodborne Illness | CDC. (2023, June 15). https://www.cdc.gov/foodborneburden/2011-foodborne-estimates.html

Cai, Y., Li, C., Wu, D., Wang, W., Tan, F., Wang, X., Wong, P. K., & Qiao, X. (2017). Highly active MgO nanoparticles for simultaneous bacterial inactivation and heavy metal removal from aqueous solution. *Chemical Engineering Journal*, *312*, 158–166. https://doi.org/10.1016/j.cej.2016.11.134

CDC. (2023, August 9). *Foodborne Illnesses and Germs*. Centers for Disease Control and Prevention. https://www.cdc.gov/foodsafety/foodborne-germs.html

CDC and Food Safety | CDC. (2023, March 15). https://www.cdc.gov/foodsafety/cdc-and-food-safety.html

Gao, W., Zhou, T., Gao, Y., Louis, B., O'Hare, D., & Wang, Q. (2017). Molten salts-modified MgO-based adsorbents for intermediate-temperature CO2 capture: A review. *Journal of Energy Chemistry*, *26*(5), 830–838. https://doi.org/10.1016/j.jechem.2017.06.005

Jung, H. S., Lee, J.-K., Kim, J.-Y., & Hong, K. S. (2003). Crystallization behaviors of nanosized MgO particles from magnesium alkoxides. *Journal of Colloid and Interface Science*, *259*(1), 127–132. https://doi.org/10.1016/S0021-9797(03)00034-1

Li, P., Lin, Y., Chen, R., & Li, W. (2020). Construction of a hierarchical-structured MgO-carbon nanocomposite from a metal–organic complex for efficient CO_2 capture and organic pollutant removal. *Dalton Transactions*, *49*(16), 5183–5191. https://doi.org/10.1039/D0DT00722F

Lin, J., Nguyen, N.-Y. T., Zhang, C., Ha, A., & Liu, H. H. (2020). Antimicrobial Properties of MgO Nanostructures on Magnesium Substrates. *ACS Omega*, *5*(38), 24613–24627. https://doi.org/10.1021/acsomega.0c03151

MacLean, R. C., & San Millan, A. (2019). The evolution of antibiotic resistance. *Science*, *365*(6458), 1082–1083. https://doi.org/10.1126/science.aax3879

Mancuso, G., Midiri, A., Gerace, E., & Biondo, C. (2021). Bacterial Antibiotic Resistance: The Most Critical Pathogens. *Pathogens*, *10*(10), Article 10. https://doi.org/10.3390/pathogens10101310

Nejati, M., Rostami, M., Mirzaei, H., Rahimi-Nasrabadi, M., Vosoughifar, M., Nasab, A. S., & Ganjali, M. R. (2022). Green methods for the preparation of MgO nanomaterials and their drug delivery, anti-cancer and anti-bacterial potentials: A review. *Inorganic Chemistry Communications*, *136*, 109107. https://doi.org/10.1016/j.inoche.2021.109107

Pepi, M., & Focardi, S. (2021). Antibiotic-Resistant Bacteria in Aquaculture and Climate Change: A Challenge for Health in the Mediterranean Area. *International Journal of Environmental Research and Public Health*, *18*(11), Article 11. https://doi.org/10.3390/ijerph18115723

USDA ERS - Cost Estimates of Foodborne Illnesses. (2023). https://www.ers.usda.gov/data-products/cost-estimates-of-foodborne-illnesses/

Vidhya, E., Vijayakumar, S., Nilavukkarasi, M., Punitha, V. N., Snega, S., & Praseetha, P. K. (2021). Green fabricated MgO nanoparticles as antimicrobial agent: Characterization and evaluation. *Materials Today: Proceedings*, *45*, 5579–5583. https://doi.org/10.1016/j.matpr.2021.02.311

Zhao, Y., Li, F., Zhang, R., Evans, D. G., & Duan, X. (2002). Preparation of Layered Double-Hydroxide Nanomaterials with a Uniform Crystallite Size Using a New Method Involving Separate Nucleation and Aging Steps. *Chemistry of Materials*, *14*(10), 4286–4291. https://doi.org/10.1021/cm020370h